Protective effect of α-mangostin against CoCl$_2$-induced apoptosis by suppressing oxidative stress in H9C2 rat cardiomyoblasts

ZHAO FANG[1], WANJUN LUO[1] and YANLI LUO[2]

[1]Department of Cardiovascular Surgery and [2]International Medical Center,
Xiangya Hospital, Central South University, Changsha, Hunan 410008, P.R. China

Abstract. *Garcinia mangostana* (a fruit) has been commonly used as a traditional drug in the treatment of various types of diseases. The aim of the present study was to evaluate the potential protective effect of α-mangostin (α-MG), a primary constituent extracted from the hull of the *G. mangostana* fruit (mangosteen), against CoCl$_2$-induced apoptotic damage in H9C2 rat cardiomyoblasts. α-MG was demonstrated to significantly improve the viability of the CoCl$_2$-treated cells by up to 79.6%, attenuating CoCl$_2$-induced damage. Further studies revealed that α-MG exerted a positive effect in terms of decreased reactive oxygen species generation, malondialdehyde concentration, cellular apoptosis, and increased superoxide dismutase activity. Furthermore, treatment with CoCl$_2$ increased the cleavage of caspase-9, caspase-3 and apoptosis regulator BAX, and reduced apoptosis regulator Bcl-2 in H9C2 cells, as measured by reverse transcription-quantitative polymerase chain reaction and western blotting, which were significantly reversed by co-treatment with α-MG (0.06 and 0.3 mM). In conclusion, these results demonstrated that α-MG protects H9C2 cells against CoCl$_2$-induced hypoxic injury, indicating that α-MG is a potential therapeutic agent for cardiac hypoxic injury.

Introduction

Ischemic heart disease (IHD), caused by myocardial ischemic injuries, frequently presents as coronary heart disease and acute myocardial infarction (1,2). IHD was reported to cause 7.4 million mortalities in 2015, and is the leading cause of mortality globally according to the World Health Organization, representing a major socioeconomic burden. Therefore, finding novel therapies to reduce the incidence of IHD is urgently required.

Previous studies demonstrated that myocardial hypoxia-ischemia is an important event during the entire process of IHD (3-5), causing extensive cardiomyocyte death (6,7). Evidence suggests that oxidative stress is involved in myocardial ischemia and that antioxidant treatment may be beneficial in cardiac damage during ischemia (7-9). Markers of oxidative stress, including reactive oxygen species (ROS), malondialdehyde (MDA) and superoxide dismutase (SOD), are frequently used to monitor mitochondrial oxidative damage (10,11). Furthermore, it has been demonstrated that apoptosis serves an important role in ischemic-hypoxic myocardial injury (12,13); when the mitochondrial membrane potential is lost, the process of apoptosis is activated, leading to cell death (14).

Garcinia mangostana is a tropical tree commonly present in Southeast Asian countries, including Vietnam, the Philippines and Thailand. The pericarp of mangosteen, the fruit of *G. mangostana*, has been used as indigenous medicine for the treatment of skin infections, wounds and diarrhea for a number of years (15,16). Previously, α-mangostin (α-MG), a major constituent extracted from the hull of mangosteen (17,18), was demonstrated to possess a variety of pharmacological properties, including anti-inflammatory (19), antitumor (20), cardioprotective (21-24), antidiabetic (25), antibacterial (26), antifungal (27), antioxidant (28) and antiobesity effects (29). α-MG has been demonstrated to arrest the cell cycle and induce apoptosis in various cancer cells via the mitochondrial pathway (20), and its prevention of cisplatin-induced apoptotic death in LLC-PK1 porcine kidney cells has been associated with the inhibition of ROS production (30). Previous *in vivo* studies have additionally demonstrated the cardioprotective effects of α-MG via the reduction of ROS generation (22-24). However, the mechanism underlying the protective effect of α-MG on cardiomyocytes remains to be fully elucidated.

CoCl$_2$, a chemical hypoxia-mimicking agent, is able to simulate the effect of ischemic-hypoxic myocardial injury (31). The H9C2 cell line is derived from rat embryonic cardiomyocytes, and may be used to investigate the electrophysiological and biochemical characteristics of myocardial tissue.

Correspondence to: Dr Yanli Luo, International Medical Center, Xiangya Hospital, Central South University, 87 Xiangya Road, Changsha, Hunan 410008, P.R. China
E-mail: lyl2211@csu.edu.cn

Myocardial cells frequently suffer from ischemic and hypoxic death during the process of cardiac surgery; therefore, the use of α-MG to potentially decrease the damage in cardiac surgery may be beneficial. To investigate this, in the present study, α-MG was added prior to $CoCl_2$ to H9C2 cells. $CoCl_2$-treated H9C2 cells were used as a model to evaluate the effects of α-MG on cardiomyoblasts exhibiting chemical hypoxia-induced injury.

Materials and methods

Materials. A Cell Counting kit-8 (CCK-8, cat no. ck04) was purchased from Dojindo Molecular Technologies, Inc., (Kumamoto, Japan). α-MG and $CoCl_2$ were purchased from Sigma-Aldrich (Merck KGaA, Darmstadt, Germany). Antibodies against apoptosis regulator Bcl-2 (rabbit anti-Bcl-2; cat no. 2870; 1:1,000), apoptosis regulator BAX (rabbit anti-Bax; cat no. 2772s; 1:1,000), rabbit anti-cleaved caspase-9 (cat no. 9507; 1:1,000), rabbit anti-cleaved caspase-3 (cat no. 9662; 1:1,000) and mouse anti-β-actin (cat. no. 3700) were purchased from Cell Signaling Technology, Inc., (Danvers, MA, USA). Annexin V/propidium iodide (PI) was purchased from BD Biosciences (Franklin Lakes, NJ, USA); and the ROS detection kit was purchased from Beyotime Institute of Biotechnology (Haimen, China).

Cell culture and treatment. H9C2 myocardial cells were purchased from the Type Culture Collection of the Chinese Academy of Sciences (Shanghai, China). Briefly, the H9C2 cells were cultured in high-glucose Dulbecco's modified Eagle's medium (Thermo Fisher Scientific, Inc., Waltham, MA, USA) containing 10% fetal bovine serum (Invitrogen; Thermo Fisher Scientific, Inc.) in 6-well plates with 5% CO_2 and 95% air at 37°C. The medium was changed every 2-3 days.

To determine the appropriate treatment conditions, chemical hypoxia was achieved by adding different concentrations of $CoCl_2$ (50, 200, 400, 600 and 800 μM) to H9C2 cells for 24 h as the preliminary experiment (32). The proper concentration was determined by the CCK-8 assay. In order to investigate the effects of α-MG following $CoCl_2$-induced cell injury, $CoCl_2$-treated H9C2 cells were maintained in complete medium with 0.012, 0.06, 0.3, 0.6 or 1.2 mM α-MG. The control cells were incubated without α-MG or $CoCl_2$.

Experimental design. According to the results of the CCK-8 assay, H9C2 cells were randomly divided into the following groups: Group I (Control), cells treated without α-MG or $CoCl_2$; group II, cells treated with $CoCl_2$ alone; group III, cells pretreated with 0.06 mM α-MG for 24 h and with $CoCl_2$ over the next 24 h; and group IV, cells pretreated with 0.3 mM α-MG for 24 h and with $CoCl_2$ over the next 24 h.

Cell viability assay. CCK-8 was used to investigate the viability of H9C2 cells cultured in 96-well plates at a density of 5,000 cells/well. When the cells had grown to 90% confluence, 600 μM $CoCl_2$ was added into the plate treated for 24 h at 37°C, then cell injury was induced. Thereafter, 10 μl CCK-8 solution was added to each well and the cells were incubated for a further 2 h at 37°C. Absorbance was measured at 450 nm with a microplate reader. The mean optical density (OD) of four wells in each group was used to calculate cell viability as follows: Cell viability (%)=($OD_{treatment\ group}$/$OD_{control\ group}$) x100.

Determination of ROS, MDA and SOD levels. The dichlorofluorescein diacetate (DCFH-DA) method was used to detect the level of intracellular ROS (33). Intracellular ROS levels were determined by measuring the oxidative conversion of cell permeable 2',7'-DCFH-DA to fluorescent dichlorofluorescein (DCF) in a BioTek Synergy 2 microplate reader (BioTek Instruments, Inc., Winooski, VT, USA). H9C2 cells were seeded (5x10^5 cells/well), α-MG (0.06 or 0.3 mM) was added to the plates for 24 h and then the $CoCl_2$-induced cell injury protocol was performed. The cells were incubated as previously described. The cells were washed with D-Hank's (Thermo Fisher Scientific, Inc.) and incubated with DCFH-DA at 37°C for 20 min. The DCF fluorescence distribution of 2x10^4 cells was detected by a microplate system at an excitation wavelength of 488 nm and an emission wavelength of 535 nm. The MDA concentration was measured by Lipid Peroxidation MDA Assay kit (Beyotime Institute of Biotechnology; cat no. S0131) and SOD activity was measured using the Superoxide Dismutase Assay kit (Beyotime Institute of Biotechnology; cat no. S0101), according to the manufacturer's protocols.

Morphological assessment of apoptotic cells by Annexin V-fluorescein isothiocyanate (FITC) and PI double staining. Apoptosis in H9C2 cells was quantified using Annexin V-FITC and PI double staining according to standard procedures using the aforementioned kit. Cell apoptosis was analyzed using CellQuest Pro software version 5.1 (BD Biosciences). Cellular fluorescence was measured by flow cytometer (FACS Calibur™, BD Biosciences).

Reverse transcription-quantitative polymerase chain reaction (RT-qPCR). Total RNA was extracted by TRIzol™ (Invitrogen; Thermo Fisher Scientific, Inc.). A total of 100 ng total RNA was used for cDNA synthesis using the Stratagene AffinityScript qPCR cDNA Synthesis kit (Agilent Technologies, Inc., Santa Clara, CA, USA). The cDNA samples were diluted 10-fold with nuclease-free H_2O and 2 μl diluted template was combined with Brilliant III Ultra-Fast SYBR® Green qPCR Master Mix (Applied Biosystems; Thermo Fisher Scientific, Inc.). β-actin was used as an internal reference control. The relative expression of target genes was determined by the $2^{-\Delta\Delta Cq}$ method (34). The qPCR cycling conditions comprised initial denaturation for 3 min at 95°C, followed by 45 cycles at 95°C (10 sec) and 58°C (45 sec); data were acquired at the end of the annealing/extension phase. Melt curve analysis was performed at the end of each run between 58 and 95°C. The gene primer sequences are exhibited in Table I. Data were analyzed using Microsoft Excel 2013 (Microsoft Corporation, Redmond, WA, USA).

Western blot analysis. Total proteins were extracted from cells using cell lysis buffer [50 mM Tris-HCl, (pH 8.0) 120 mM NaCl; 0.5% NP-40; 1 mM phenylmethylsulfonyl fluoride] and determined using bicinchoninic acid assay. A total of 40 μg protein extract was separated by 12% SDS-PAGE, followed by transfer to a polyvinylidene difluoride membrane

Table I. Primer sequences of Bcl-2, Bax, caspase-3, caspase-9 and β-actin.

Gene	Primer sequences
Bcl-2	FP: 5'-GGATGACTGAGTACCTGAA-3'
	RP: 5'-GCCATATAGTTCCACAAAGG-3'
Bax	FP: 5'-GATGAACTGGACAACAACAT-3'
	RP: 5'-CACGGAAGAAGACCTCTC-3'
Caspase-3	FP: 5'-ATTATGGAATTGATGGATAGTGTT-3'
	RP: 5'-GTAGTCGCCTCTGAAGAA-3'
Caspase-9	FP: 5'-ACTGCCTCATCATCAACA-3'
	RP: 5'-GTTCTTCACCTCCACCAT-3'
β-actin	FP: 5'-CGTAAAGACCTCTATGCCAACA-3'
	RP: 5'-AGCCACCAATCCACACAGAG-3'

FP, forward primer; RP, reverse primer; Bax, apoptosis regulator BAX; Bcl-2, apoptosis regulator Bcl-2.

Figure 1. H9C2 cells were incubated with different concentrations of $CoCl_2$ for 24 h, and cell viability was analyzed by Cell Counting kit-8 assay. Results are expressed as the mean ± standard error of the mean (n=3). *$P<0.05$, **$P<0.01$ and ***$P<0.001$ vs. control.

Figure 2. H9C2 cells were incubated with different concentrations of α-MG for 24 h prior to $CoCl_2$-induced injury, and cell viability was analyzed by Cell Counting kit-8 assay. Results are expressed as the mean ± standard error of the mean (n=3). ***$P<0.001$ vs. control; #$P<0.05$, ##$P<0.01$ and ###$P<0.001$ vs. $CoCl_2$-induced injury group; △△$P<0.01$ and △△△$P<0.001$ vs. 0.06 mM α-MG-treated group. α-MG, α-mangostin.

(Bio-Rad Laboratories, Inc.), blocking with 5% non-fat milk in TBS-Tween buffer 7 (0.12 M Tris-base, 1.5 M NaCl, 0.1% Tween-20) for 1 h at room temperature, and incubation with the appropriate antibodies including rabbit anti-Bcl-2 (cat no. 2870; 1:1,000), rabbit anti-Bax (cat no. 2772s; 1:1,000), rabbit anti-cleaved caspase-9 (cat no. 9507; 1:1,000), rabbit anti-cleaved caspase-3 (cat no. 9662; 1:1,000) and mouse anti-actin (cat no. 3700) were purchased from Cell Signaling Technology, Inc., (Danvers, MA, USA), overnight at 4°C. Subsequently, the blots were incubated with horseradish peroxidase-conjugated anti-rabbit secondary antibody (1:10,000; cat no. 111-035-003; Jackson Immunoresearch Laboratories, Inc., West Grove, PA, USA) for 30 min at room temperature. The bound antibodies were detected using a chemiluminescence (ECL) system and autoradiography (cat. no. PI32209; Pierce; Thermo Fisher Scientific, Inc.). Quantity One analysis software version 4.6.9 (Bio-Rad Laboratories, Inc., Hercules, CA, USA) was used to quantify the relative band intensities from western blot images.

Caspase-3 and caspase-9 activity assay. The activity of caspase-3 and caspase-9 was determined using a Caspase-3 Activity Assay kit and a Caspase-9 Activity Assay kit (Beyotime Institute of Biotechnology). This assay is based on the detection of the chromophore p-nitroaniline (pNA) by spectrophotometry following cleavage of pNA from the substrate by caspase-3/caspase-9. Assays were performed in 96-well plates ($5x10^4$ cells/well), with each well containing 10 μl protein cell lysate, 80 μl reaction buffer and 10 μl substrate (Asp-Glu-Val-Asp-pNA for caspase-3 and Leu-Glu-His-Asp-pNA for caspase-9). The results were quantified spectrophotometrically using a BioTek Synergy 2 microplate reader (BioTek Instruments, Inc.) at a wavelength of 405 nm. Caspase activity was presented as a percentage relative to the control group.

Statistical analysis. The results are reported as the mean ± standard error of the mean for at least three analyses
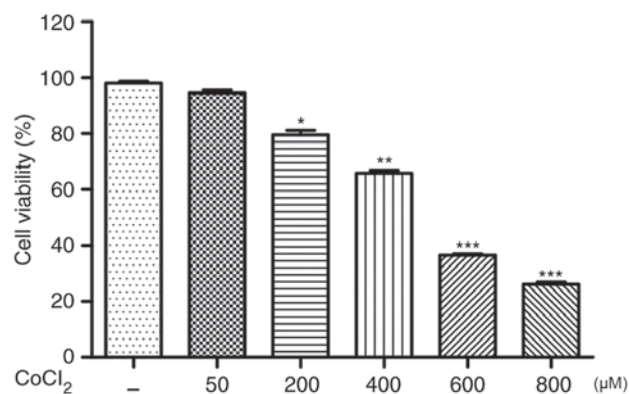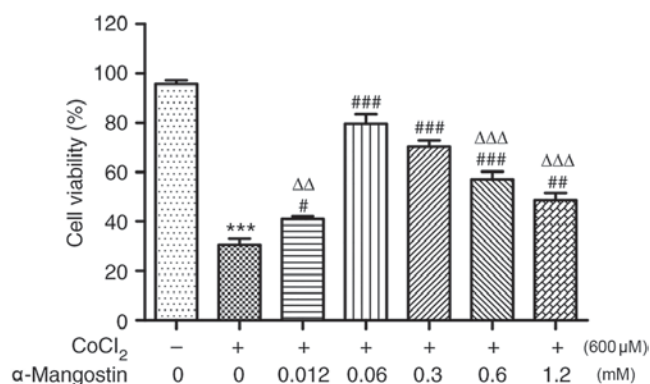
for each sample. Quantitative variables were compared using one-way analysis of variance to compare differences in two or more groups, and the Tukey test was performed for post-hoc subgroup analysis, as appropriate. Statistical analysis was performed using the SPSS 19.0 software package (IBM Corp., Armonk, NY, USA) and GraphPad Prism 5.0 (GraphPad Software, Inc., La Jolla, CA, USA). $P<0.05$ was considered to indicate a statistically significant difference.

Results

Effect of α-MG on $CoCl_2$-induced cell viability. As exhibited in Fig. 1, H9C2 cells treated with $CoCl_2$ (≥600 μM) for 24 h exhibited significantly reduced cell viability ($P<0.001$). The choice of 600 μM for the concentration of $CoCl_2$ applied to all experiments was based on these results from the CCK-8 assay. However, in H9C2 cells pretreated with various concentrations of α-MG, $CoCl_2$-induced hypoxic injury was significantly reduced ($P<0.05$; Fig. 2). Cells pretreated with α-MG at concentrations between 0 and 12 mM presented as an 'inverted U shape' in the present study: At concentrations of 0.012-0.06 mM, cell viability increased gradually ($P<0.05$),
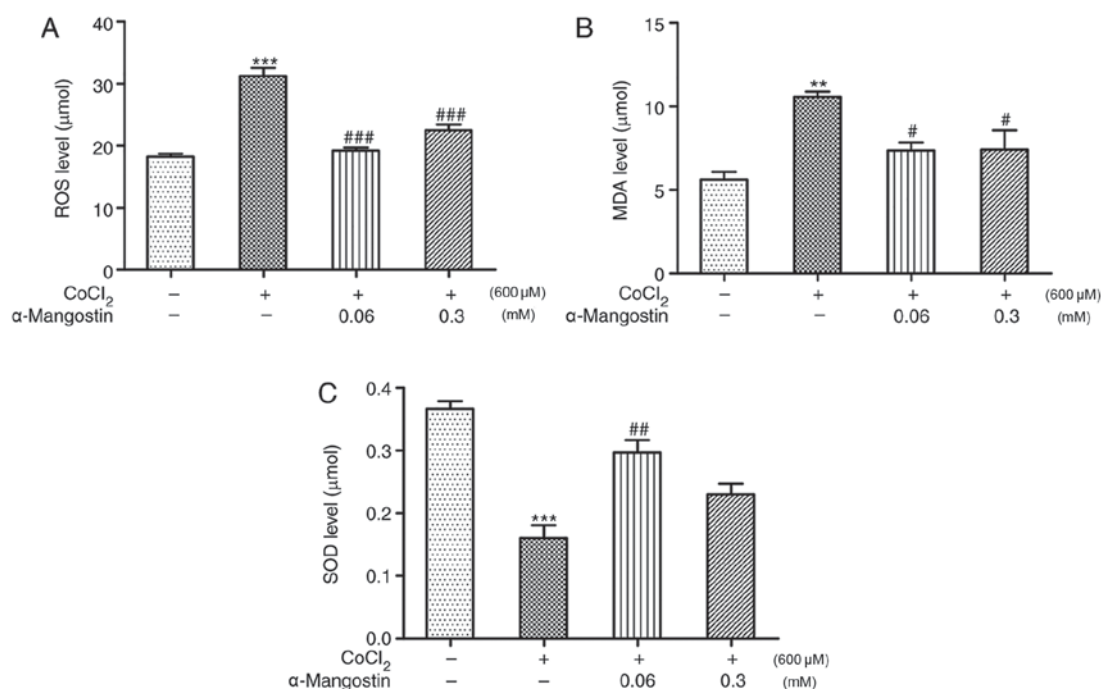
Figure 3. H9C2 cells were incubated with α-MG (0.06 or 0.3 mM) for 24 h prior to CoCl$_2$-induced injury and the effects of CoCl$_2$ on ROS production, MDA concentration and SOD activity were assessed. (A) Results of the ROS assay. (B) Results of the MDA assay. (C) Results of the SOD assay. Each bar represents the mean ± standard error of the mean (n=3). **P<0.01 and ***P<0.001 vs. control group; #P<0.05, ##P<0.01 and ###P<0.001 vs. CoCl$_2$-induced injury group. α-MG, α-mangostin; ROS, reactive oxygen species; SOD, superoxide dismutase; MDA, malondialdehyde.

reaching a maximum at 0.06 mM; at concentrations of 0.06-1.2 mM the curve exhibited a steep decline, indicating a decrease in cell viability with increasing concentrations, although cell viability remained higher compared with the group treated with CoCl$_2$ alone (P<0.05). Among the α-MG pretreatment groups, all exhibited significant differences compared with the 0.06 mM group (P<0.01), apart from the 0.3 mM group (P>0.05).

Effects of α-MG on CoCl$_2$-induced alterations in ROS generation, MDA concentration and SOD activity. The involvement of ROS in the CoCl$_2$-induced apoptosis of H9C2 cells was evaluated by measuring the level of ROS production. Following treatment of H9C2 cells with 600 µM CoCl$_2$ for 24 h, the intracellular ROS level increased significantly compared with that in the control group (P<0.001). However, treatment with α-MG decreased the intracellular ROS levels significantly (P<0.001), further demonstrating its antioxidant effects (Fig. 3A). As exhibited in Fig. 3B and C, H9C2 cells treated with CoCl$_2$ exhibited significantly increased MDA concentrations and reduced SOD concentration (P<0.01 and P<0.001, respectively). The oxidative abnormalities were ameliorated by α-MG at a concentration of 0.06 mM, as demonstrated by the significant reduction in MDA concentration and the increase in SOD activity (P<0.05).

Effects of α-MG on CoCl$_2$-induced cell apoptosis. To further investigate the functional effect of α-MG in H9C2 cells treated with CoCl$_2$, cellular apoptosis in H9C2 cells was assessed using the Annexin V-FITC/PI method with flow cytometry. The results demonstrated that CoCl$_2$ increased the percentage

of apoptotic H9C2 cells to ~60%, which was attenuated by treatment with 0.06 mM α-MG (reduced to ~5.8%) and 0.3 mM α-MG (P<0.001; reduced to ~15.34%), indicating the cytoprotective effect of α-MG against chemical hypoxia-induced apoptosis (Fig. 4).

Effect of α-MG on cell apoptosis-regulating genes. The results of the RT-qPCR (Fig. 5) revealed that treatment with CoCl$_2$ significantly decreased the expression level of Bcl-2 to 64.9% and increased the expression levels of Bax, caspase-9 and caspase-3 to 194, 138 and 193% relative to the control group, respectively (P<0.001 vs. control group). However, pretreatment with α-MG at a concentration of 0.06 mM increased the expression level of Bcl-2 to 81.4% and attenuated the expression levels of Bax, caspase-9 and caspase-3 to 110, 120 and 133% relative to the control group, respectively (P<0.001 vs. CoCl$_2$-induced injury group), while pretreatment with α-MG at a concentration of 0.3 mM increased the expression level of Bcl-2 to 70.8% and attenuated the expression levels of Bax, caspase-9 and caspase-3 to 142, 126 and 182% relative to the control group, respectively (P<0.05 vs. CoCl$_2$-induced injury group).

Effect of α-MG on cellular apoptosis-regulating protein expression. As depicted in Fig. 6, protein expression was analyzed by western blotting. Treatment with CoCl$_2$ significantly downregulated the expression level of Bcl-2 to 49.6% and upregulated the levels of Bax, caspase-9 and caspase-3 to 285, 1,111 and 307% relative to the control group, respectively (P<0.001). Pretreatment with α-MG at a concentration of 0.06 mM upregulated the expression level of Bcl-2 to 87.6% and downregulated the expression levels of Bax, caspase-9
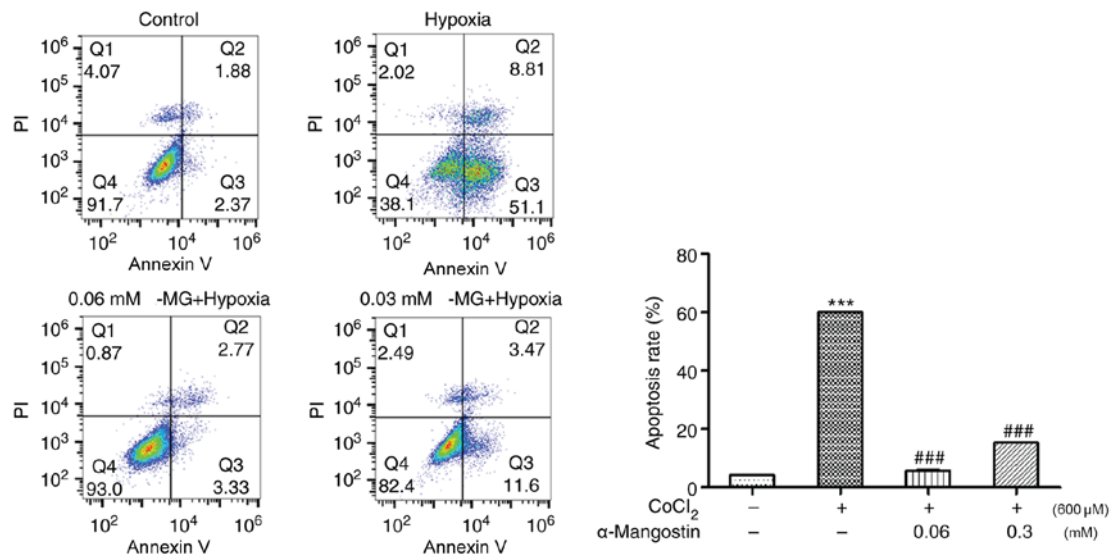
Figure 4. H9C2 cells were incubated with α-MG (0.06 or 0.3 mM) for 24 h prior to CoCl$_2$-induced injury and cells were stained with PI/Annexin V-fluorescein isothiocyanate and analyzed by fluorescence-activated cell sorting. The results are expressed as the mean ± standard error of the mean (n=3). ***P<0.001 vs. the control group; ###P<0.001 vs. CoCl$_2$-induced injury group. α-MG, α-mangostin; PI, propidium iodide.
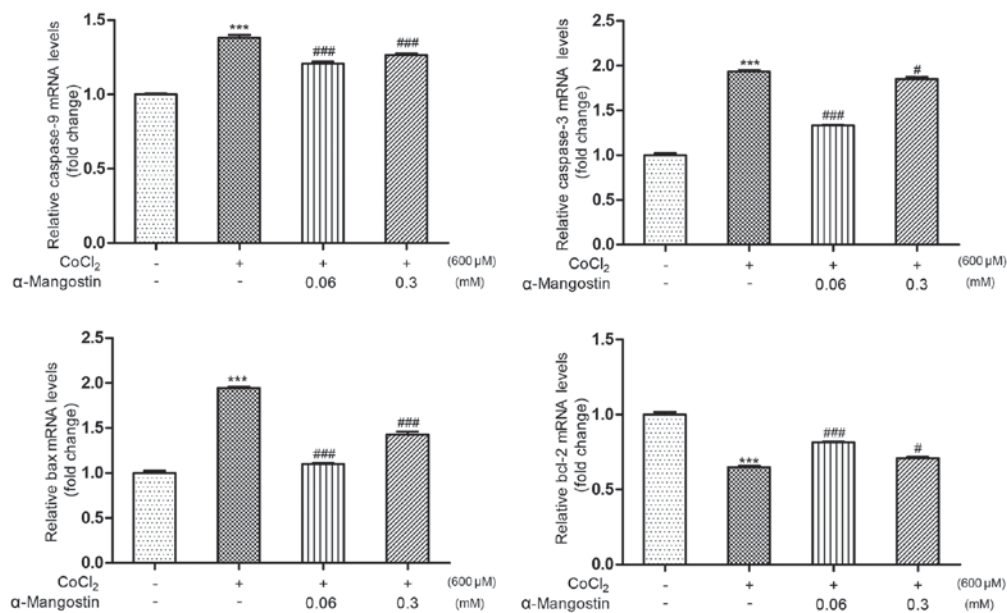

Figure 5. Effect of treatment with α-MG on CoCl$_2$-induced apoptosis in H9C2 cells as assessed by RT-qPCR. The expression levels of Bax, Bcl-2, caspase-9 and caspase-3 were analyzed by RT-qPCR. Each bar represents the mean ± standard error of the mean (n=3). ***P<0.001 vs. the control group; #P<0.05 and ###P<0.001 vs. CoCl$_2$-induced injury group. α-MG, α-mangostin; RT-qPCR, reverse transcription-quantitative polymerase chain reaction; Bax, apoptosis regulator BAX; Bcl-2, apoptosis regulator Bcl-2.

and caspase-3 to 138, 474 and 157%, respectively (P<0.01), while pretreatment with α-MG at a concentration of 0.3 mM downregulated the expression levels of Bax, caspase-9 and caspase-3 to 165, 650 and 183%, respectively (P<0.01), while there was not significant difference with Bcl-2.

Effect of α-MG on the activation of caspase-3 and caspase-9. The activation of caspase-3 and caspase-9 has important influences on apoptosis. When compared with the control group (Fig. 7), treatment with CoCl$_2$ significantly increased the activity of caspase-3 and caspase-9 to 270 and 906%, respectively (P<0.001). When pretreated with α-MG (0.06 and 0.3 mM),

the activities of caspase-3 (140 and 167%, respectively) and caspase-9 (447 and 573%, respectively) were significantly attenuated (P<0.001 vs. CoCl$_2$-induced injury group).

Discussion

The findings of the present study revealed that α-MG, a promising cardioprotective natural extract, was able to suppress oxidative stress and inhibit apoptosis in H9C2 cells by attenuating cellular oxidative damage. To the best of the authors' knowledge, this is the first report describing the anti-apoptotic effect of α-MG in H9C2 cells.
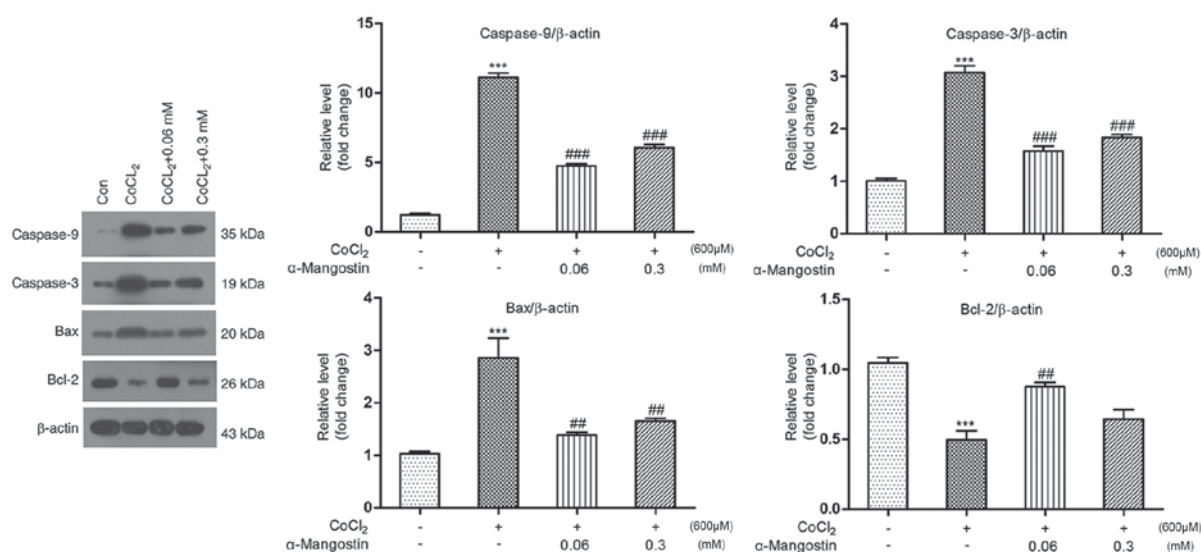
Figure 6. Effect of treatment with α-MG on CoCl₂-induced apoptosis in H9C2 cells as assessed by western blotting. The expression levels of Bax, Bcl-2, caspase-9 and caspase-3 were analyzed by western blotting. Each bar represents the mean ± standard error of the mean (n=3). ***P<0.001 vs. the control group; ##P<0.01 and ###P<0.001 vs. CoCl₂-induced injury group. α-MG, α-mangostin; Bax, apoptosis regulator BAX; Bcl-2, apoptosis regulator Bcl-2.
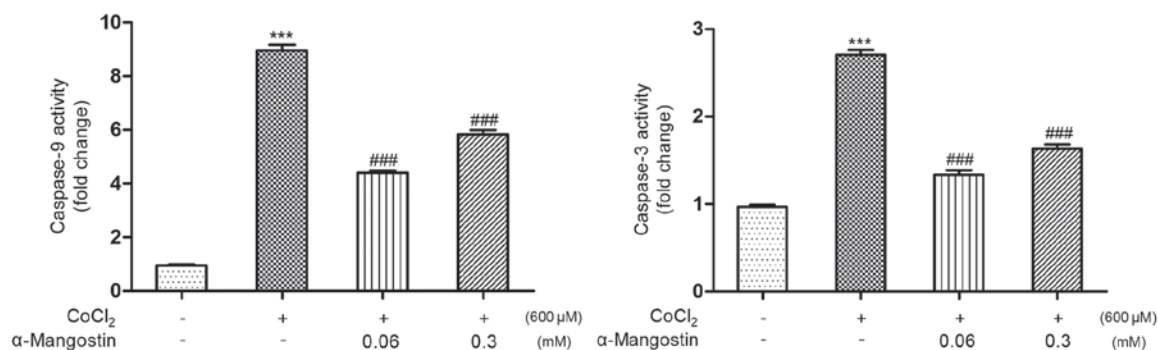

Figure 7. Effect of treatment with α-MG on the activity of caspase-3 and caspase-9 in H9C2 cells, as determined using commercial caspase-3/caspase-9 activity assay kits. Each bar represents the mean ± standard error of the mean (n=3). ***P<0.001 vs. control group; ###P<0.001 vs. CoCl₂-induced injury group. α-MG, α-mangostin.

Mangosteen fruit has been used for centuries to alleviate a number of pathological conditions in humans. In 1855, α-MG was identified among the major xanthones isolated from the pericarp of the mangosteen fruit (35). This compound is yellowish in color and may additionally be obtained from other parts of the plant. The structure of this xanthone was interpreted by Dragendorff [reviewed in (36)]. The molecular formula, type and position of the substituent groups of α-MG were subsequently determined by Stout *et al* (37). Preclinical studies with purified α-MG, the major constituent of the pericarp of mangosteen, have demonstrated its beneficial effects in various diseases. However, the cardioprotective effects of α-MG have not been extensively investigated. In a study conducted by Devi Sampath and Vijayaraghavan (22), rats were administered oral α-MG at a dose of 200 mg/kg prior to the induction of myocardial infarction by isoproterenol (ISO). On comparing the experimental groups, the myocardial injury markers and oxidation products were increased significantly in the blood and myocardia of rats not treated with oral α-MG, whereas they were significantly reduced in rats with myocardial injury that received oral α-MG, demonstrating that α-MG exerts a protective effect against lipid peroxidation

and enhances the antioxidant tissue defense system during ISO-induced myocardial infarction in rats. A further study on the activity of rat myocardium mitochondrial enzymes revealed significantly increased enzyme activity, indicating mitochondrial damage, following treatment with ISO in rats that did not receive oral α-MG, whereas oral α-MG was able to reverse this result, suggesting that α-MG may reduce the occurrence of ISO-induced myocardial infarction, mitochondrial dysfunction and associated oxidative stress (23). Buelna-Chontal *et al* (24) reported that α-MG exerts a protective effect in the post-ischemic heart, which is associated with the prevention of oxidative stress secondary to reperfusion injury. To date, studies have focused on animal research, whereas a study *in vitro* has not been reported.

Hypoxia may induce ROS generation and lipid peroxidation (38). ROS, a series of cellular molecules generated during oxygen metabolism, are generally considered to be important mediators of oxidative stress injury (39). The MDA concentration frequently reflects the degree of lipid peroxidation, indirectly reflecting the degree of cellular oxidative injury (40). SOD decrease cellular free oxygen radicals (41). The present study demonstrated that the ROS level and MDA concentration

were increased in H9C2 cells treated with $CoCl_2$, while the activity of SOD was suppressed. In H9C2 cells treated with α-MG, the results were reversed, demonstrating the antioxidant effects of α-MG, which coincide with the observations *in vivo*.

It was previously reported that apoptosis is rare in the healthy myocardium, with a percentage of 0.001-0.002% (42); however, when the cells become damaged, they may undergo apoptosis. Oxidative stress usually causes DNA damage, and instability of the membrane, cellular lipids and proteins, leading to cellular dysfunction and apoptosis (43). In the present study, myocardial cell viability decreased following treatment with $CoCl_2$, and the apoptosis rate increased. α-MG-treated groups (at concentrations of 0.06 and 0.3 mM) exhibited decreased oxidative stress and apoptosis rates, indicating the protective effect of α-MG against $CoCl_2$-induced apoptosis.

The first limitation of the present study is associated with the use of $CoCl_2$, which is commonly used for constructing hypoxic models in different cell lines (44,45). $CoCl_2$-treated cells were used as a model of chemical hypoxia-induced injury; however, there are several other effects of hypoxia that are not achieved by treatment with $CoCl_2$. For example, $CoCl_2$ may stabilize the expression of hypoxia-inducible factor 1α (HIF-1α) (46,47). Second, the mechanisms underlying the antioxidant and anti-apoptotic properties of α-MG are not fully elucidated, and continued research is required in the future.

In conclusion, in the present study, a myocardial cell model of hypoxia was successfully constructed and α-MG was demonstrated to be effective in reducing apoptosis and oxidative stress induced by $CoCl_2$.

Acknowledgements

Funding

Availability of data and materials

All data generated or analyzed during the present study are included in this published article.

Authors' contributions

FZ contributed to acquisition, analysis and interpretation of data, writing the main manuscript text, LYL and LWJ designed the study and contributed by revising the manuscript.

Ethics approval and consent to participate

Not applicable.

Consent for publication

Not applicable.

Competing interests

The authors declare that they have no competing interests.

References

1. Luo D, Yao YY, Li YF, Sheng ZL, Tang Y, Fang F, Fang K, Ma GS and Teng GJ: Myocardial infarction quantification with late gadolinium-enhanced magnetic resonance imaging in rats using a 7-T scanner. Cardiovasc Pathol 21: 112-119, 2012.
2. Shibata R, Sato K, Pimentel DR, Takemura Y, Kihara S, Ohashi K, Funahashi T, Ouchi N and Walsh K: Adiponectin protects against myocardial ischemia-reperfusion injury through AMPK- and COX-2-dependent mechanisms. Nat Med 11: 1096-1103, 2005.
3. Wu LX, Gu XF, Zhu YC and Zhu YZ: Protective effects of novel single compound, Hirsutine on hypoxic neonatal rat cardiomyocytes. Eur J Pharmacol 650: 290-297, 2011.
4. Zhang J, Liu A, Hou R, Zhang J, Jia X, Jiang W and Chen J: Salidroside protects cardiomyocyte against hypoxia-induced death: A HIF-1alpha-activated and VEGF-mediated pathway. Eur J Pharmacol 607: 6-14, 2009.
5. Zhu HM and Deng L: Evaluation of cardiomyocyte hypoxia injury models for the pharmacological study in vitro. Pharm Biol 50: 167-174, 2012.
6. Sharov VG, Todor AV and Sabbah HN: Left ventricular histomorphometric findings in dogs with heart failure treated with the acorn cardiac support device. Heart Fail Rev 10: 141-147, 2005.
7. Ibáñez B, Heusch G, Ovize M and Van de Werf F: Evolving therapies for myocardial ischemia/reperfusion injury. J Am Coll Cardiol 65: 1454-1471, 2015.
8. Xie Q, Li XX, Zhang P, Li JC, Cheng Y, Feng YL, Huang BS, Zhuo YF and Xu GH: Hydrogen gas protects against serum and glucose deprivation-induced myocardial injury in H9c2 cells through activation of the NF-E2-related factor 2/heme oxygenase 1 signaling pathway. Mol Med Rep 10: 1143-1149, 2014.
9. Li T, Zhang P, Liu J, Zhou R, Li Q, You Z and Dian K: Protective effects of hemoglobin-based oxygen carrier given to isolated heart during ischemia via attenuation of mitochondrial oxidative damage. Free Radic Biol Med 48: 1079-1089, 2010.
10. Dou MM, Zhang ZH, Li ZB, Zhang J and Zhao XY: Cardioprotective potential of Dendrobium officinale Kimura et Migo against myocardial ischemia in mice. Mol Med Rep 14: 4407-4414, 2016.
11. Yang Y, Duan W, Jin Z, Yi W, Yan J, Zhang S, Wang N, Liang Z, Li Y, Chen W, *et al*: JAK2/STAT3 activation by melatonin attenuates the mitochondrial oxidative damage induced by myocardial ischemia/reperfusion injury. J Pineal Res 55: 275-286, 2013.
12. Gallo S, Gatti S, Sala V, Albano R, Costelli P, Casanova E, Comoglio PM and Crepaldi T: Agonist antibodies activating the Met receptor protect cardiomyoblasts from cobalt chloride-induced apoptosis and autophagy. Cell Death Dis 5: e1185, 2014.
13. Pyo JO, Nah J, Kim HJ, Chang JW, Song YW, Yang DK, Jo DG, Kim HR, Chae HJ, Chae SW, *et al*: Protection of cardiomyocytes from ischemic/hypoxic cell death via Drbp1 and pMe2GlyDH in cardio-specific ARC transgenic mice. J Biol Chem 283: 30707-30714, 2008.
14. Hausenloy DJ and Yellon DM: The mitochondrial permeability transition pore: Its fundamental role in mediating cell death during ischaemia and reperfusion. J Mol Cell Cardiol 35: 339-341, 2003.
15. Nagy S and Shaw PE: Tropical and subtropical fruits: Composition, properties and uses. Mol Nut 25: 582, 1980.
16. Gupta KK, Khandelwal G, Prasad G, Chopra AK and Mishra A: A review on scientific technologies in practice to innovate plant based molecules and to improve herbal drug quality to overcome health problems. J App Nat Sci 2: 165-181, 2010.
17. Gopalakrishnan G and Balaganesan B: Two novel xanthones from *Garcinia mangostana*. Fitoterapia 71: 607-609, 2000.
18. Suksamrarn S, Suwannapoch N, Ratananukul P, Aroonlerk N and Suksamrarn A: Xanthones from the green fruit hulls of *Garcinia mangostana*. J Nat Prod 65: 761-763, 2002.
19. Chomnawang MT, Surassmo S, Nukoolkarn VS and Gritsanapan W: Effect of *Garcinia mangostana* on inflammation caused by *Propionibacterium acnes*. Fitoterapia 78: 401-408, 2007.

20. Matsumoto K, Akao Y, Ohguchi K, Ito T, Tanaka T, Iinuma M and Nozawa Y: Xanthones induce cell-cycle arrest and apoptosis in human colon cancer DLD-1 cells. Bioorg Med Chem 13: 6064-6069, 2005.
21. Jiang DJ, Dai Z and Li YJ: Pharmacological effects of Xanthones as cardiovascular protective agents. Cardiovasc Drug Rev 22: 91-102, 2004.
22. Devi Sampath P and Vijayaraghavan K: Cardioprotective effect of alpha-mangostin, a xanthone derivative from mangosteen on tissue defense system against isoproterenol-induced myocardial infarction in rats. J Biochem Mol Toxicol 21: 336-339, 2007.
23. Sampath PD and Kannan V: Mitigation of mitochondrial dysfunction and regulation of eNOS expression during experimental myocardial necrosis by alpha-mangostin, a xanthonic derivative from *Garcinia mangostana*. Drug Chem Toxicol 32: 344-352, 2009.
24. Buelna-Chontal M, Correa F, Hernández-Reséndiz S, Zazueta C and Pedraza-Chaverri J: Protective effect of α-mangostin on cardiac reperfusion damage by attenuation of oxidative stress. J Med Food 14: 1370-1374, 2011.
25. Kumar V, Bhatt PC, Kaithwas G, Rashid M, Al-abbasi FA, Khan JAJ, Anwar F and Verma A: α-mangostin mediated pharmacological modulation of hepatic carbohydrate metabolism in diabetes induced wistar rat. Beni-Suef Uni J Basic App Sci 5: 255-276, 2016.
26. Iinuma M, Tosa H, Tanaka T, Asai F, Kobayashi Y, Shimano R and Miyauchi K: Antibacterial activity of xanthones from guttiferaeous plants against methicillin-resistant Staphylococcus aureus. J Pharm Pharmacol 48: 861-865, 1996.
27. Kaomongkolgit R, Jamdee K and Chaisomboon N: Antifungal activity of alpha-mangostin against *Candida albicans*. J Oral Sci 51: 401-406, 2009.
28. Williams P, Ongsakul M, Proudfoot J, Croft K and Beilin L: Mangostin inhibits the oxidative modification of human low density lipoprotein. Free Radic Res 23: 175-184, 1995.
29. Quan X, Wang Y, Ma X, Liang Y, Tian W, Ma Q, Jiang H and Zhao Y: α-Mangostin induces apoptosis and suppresses differentiation of 3T3-L1 cells via inhibiting fatty acid synthase. PLoS One 7: e33376, 2012.
30. Lee D, Choi YO, Kim KH, Chin YW, Namgung H, Yamabe N and Jung K: Protective effect of α-mangostin against iodixanol-induced apoptotic damage in LLC-PK1 cells. Bioorg Med Chem Lett 26: 3806-3809, 2016.
31. Goldberg MA, Dunning SP and Bunn HF: Regulation of the erythropoietin gene: Evidence that the oxygen sensor is a heme protein. Science 242: 1412-1415, 1988.
32. Park JK, Jeong JW, Kang MY, Baek JC, Shin JK, Lee SA, Choi WS, Lee JH and Paik WY: Inhibition of the PI3K-Akt pathway suppresses sFlt1 expression in human placental hypoxia models in vitro. Placenta 31: 621-629, 2010.
33. Jia SJ, Jiang DJ, Hu CP, Zhang XH, Deng HW and Li YJ: Lysophosphatidylcholine-induced elevation of asymmetric dimethylarginine level by the NADPH oxidase pathway in endothelial cells. Vascul Pharmacol 44: 143-148, 2006.
34. Livak KJ and Schmittgen TD: Analysis of relative gene expression data using real-time quantitative PCR and the 2(-Delta Delta C(T)) method. Methods 25: 402-408, 2001.
35. Schmid W: Ueber das Mangostin. Eur J Org Chem 93: 83-88, 1855.
36. Ibrahim MY, Hashim NM, Mariod AA, Mohan S, Abdulla MA, Abdelwahab SI and Arbab IA: α-Mangostin from *Garcinia mangostana* Linn: An updated review of its pharmacological properties. Arabian J Chem 9: 317-329, 2016.
37. Stout GH, Krahn MM, Yates P and Bhat HB: The structure of mangostin. Chem Commun 4: 211-212, 1968.
38. Chang ST, Chung CM, Chu CM, Yang TY, Pan KL, Hsu JT and Hsiao JF: Platelet glycoprotein IIb/IIIa inhibitor tirofiban ameliorates cardiac reperfusion injury. Int Heart J 56: 335-340, 2015.
39. Schieber M and Chandel NS: ROS function in redox signaling and oxidative stress. Curr Biol 24: R453-R462, 2014.
40. Del Rio D, Stewart AJ and Pellegrini N: A review of recent studies on malondialdehyde as toxic molecule and biological marker of oxidative stress. Nutr Metab Cardiovasc Dis 15: 316-328, 2005.
41. Liu J, Hou J, Xia ZY, Zeng W, Wang X, Li R, Ke C, Xu J, Lei S and Xia Z: Recombinant PTD-Cu/Zn SOD attenuates hypoxia-reoxygenation injury in cardiomyocytes. Free Radic Res 47: 386-393, 2013.
42. Wang Y, Gong GH, Xu YN, Yu LJ and Wei CX: Sugemule-3 protects against isoprenaline-induced cardiotoxicity in vitro. Pharmacogn Mag 13: 517-522, 2017.
43. Moris D, Spartalis M, Tzatzaki E, Spartalis E, Karachaliou GS, Triantafyllis AS, Karaolanis GI, Tsilimigras DI and Theocharis S: The role of reactive oxygen species in myocardial redox signaling and regulation. Ann Transl Med 5: 324, 2017.
44. Dai ZJ, Gao J, Ma XB, Yan K, Liu XX, Kang HF, Ji ZZ, Guan HT and Wang XJ: Up-regulation of hypoxia inducible factor-1α by cobalt chloride correlates with proliferation and apoptosis in PC-2 cells. J Exp Clin Cancer Res 31: 28, 2012.
45. Grasselli F, Basini G, Bussolati S and Bianco F: Cobalt chloride, a hypoxia-mimicking agent, modulates redox status and functional parameters of cultured swine granulosa cells. Reprod Fertil Dev 17: 715-720, 2005.
46. Srinivasan S and Dunn JF: Stabilization of hypoxia-inducible factor-1α in buffer containing cobalt chloride for Western blot analysis. Anal Biochem 416: 120-122, 2011.
47. Huang BW, Miyazawa M and Tsuji Y: Distinct regulatory mechanisms of the human ferritin gene by hypoxia and hypoxia mimetic cobalt chloride at the transcriptional and post-transcriptional levels. Cell Signal 26: 2702-2709, 2014.